


A network-based dynamic air traffic flow model for short-term en route traffic prediction

Dan Chen* , Minghua Hu, Yuanyuan Ma and Jianan Yin

College of Civil Aviation, Nanjing University of Aeronautics and Astronautics, Nanjing, China

SUMMARY

This paper presents a dynamic network-based approach for short-term air traffic flow prediction in en route airspace. A dynamic network characterizing both the topological structure of airspace and the dynamics of air traffic flow is developed, based on which the continuity equation in fluid mechanics is adopted to describe the continuous behaviour of the en route traffic. Building on the network-based continuity equation, the space division concept in cell transmission model is introduced to discretize the proposed model both in space and time. The model parameters are sequentially updated based on the statistical properties of the recent radar data and the new predicting results. The proposed method is applied to a real data set from Shanghai Area Control Center for the short-term air traffic flow prediction both at flight path and en route sector level. The analysis of the case study shows that the developed method can characterize well the dynamics of the en route traffic flow, thereby providing satisfactory prediction results with appropriate uncertainty limits. The mean relative prediction errors are less than 0.10 and 0.14, and the absolute errors fall in the range of 0 to 1 and 0 to 3 in more than 95% time intervals respectively, for the flight path and en route sector level. Copyright © 2017 John Wiley & Sons, Ltd.

KEY WORDS: airspace dynamic network; short-term prediction; aggregate model; en route traffic dynamics; travel time distributions

1. INTRODUCTION

Air traffic in China has grown uninterruptedly during the last few decades, whose annual growth rate has reached 9% and cumulative growth has passed 60% from 1960s up to now [1]. A recent study suggests that the anticipated annual growth of air traffic is 5.8% in the next 20 years [2]. Realizing the problem brought by the increased air traffic flow and limited airspace, the Chinese government plans to improve the air traffic flow management (ATFM) system to address the demand–capacity unbalance problem. In the public literature, many air traffic flow models have been developed to describe the traffic flow in the specified airspace and to forecast the trend in the short term, which can be further used for decision-making and evaluation of the various control strategies [3–13, 18–24]. The air traffic flow models were put in the semi-automated ATFM system to assist the air traffic controllers in alleviating en route air traffic congestion by making control strategies in advance, which will thus balance the demand and capacity in a more efficient manner.

Current literatures reveal that there are mainly two air traffic modelling methods, trajectory-based method and aggregate method [3–13, 18–24]. The trajectory-based model is widely used in the US air traffic control system for traffic demand forecasting. Trajectory-based air traffic flow forecast is carried out by counting the total number of aircraft in a specified airspace by propagating the trajectories of the proposed flights forward in time [3, 4]. But recent research reveals that the errors of the trajectory-based flow prediction increase sharply when the forecast time horizon exceeds 20 minutes, which can be attributed to its sensitivity to various uncertainty factors, such as the weather factors,

*Correspondence to: Dan Chen, College of Civil Aviation, Nanjing University of Aeronautics and Astronautics, 29 Jiangjun Road, Jiangning, Nanjing 211106, China. E-mail: chendan2011@nuaa.edu.cn

airport conditions, airline operation and human factors. [4]. Furthermore, the dimension of the model depends on the number of aircraft under consideration, which demands a huge computational cost in real context to resolve. Thus, in practice, it is difficult to make sound online air traffic control strategies based on the trajectory-based model due to the short forecast horizon and the expensive computational cost.

Efficient ATFM requires reasonable prediction of the whole traffic flow situations in the specified airspace, rather than the temporal–spatial information of individual aircraft. Therefore, the aggregate air traffic flow models are introduced recently, which focus on the overall distribution of the air traffic flow in the airspace volumes of interest [5–13, 18–24]. Because the aircrafts in the airspace volumes are spatially aggregated, the dimension of the aggregated model depends solely on the number of airspace volumes rather than the total number of aircrafts in the airspace, which will reduce the computational cost significantly. In addition, because the behaviour of the individual aircraft is not taken into account in the aggregated model, it is less sensitive to the uncertainty factors related to individual aircraft, such as the departure delay and the weather, and thus, a longer forecast time horizon with less prediction errors can be achieved.

Recently, the aggregated approach is widely discussed in the literatures [5–13, 18–24]. A stochastic framework with linear dynamic system model was developed by Sridhar *et al.*, where the dimension of the model depends on the number of control volumes by introducing split parameters to describe the air traffic flow distribution in neighbouring airspace. The time-invariant model proposed is further developed into a time-variant one, in which the parameters are updated every 1 hour based on the historical air traffic operational data [5, 6]. And then Gilbo *et al.* and Sridhar *et al.* further explored the stochastic linear dynamic system model to predict the air traffic flow at the sector and the centre levels [7, 8]. Michael *et al.* extended the previous model by adapting quadratic cost on cumulative departure delays to analyse pre-departure delay distribution across the National Airspace System [9]. Shon *et al.* and Giovanni *et al.* proposed a linear programming model on the basis of the aggregate model to make optimal congestion management strategies [10–12]. The major shortcoming of the stochastic framework is that it adopts Poisson distributions to model the departures at each time step, ignoring the fact that the departure traffic flow varies significantly during days, weeks and seasons under different traffic conditions. The other point is that the split parameters cause the diffusion and dispersion problem, which may result in inaccurate predictions [13]. On the other hand, motivated by the widely used LWR theory (traffic flow theory proposed by Lighthill, Whitham and Richards) [14, 15] and the cell transmission model [16, 17] in highway traffic modelling, Menon *et al.* derived the aggregate air traffic model from the Eulerian model [18]. Then, the derived one-dimension model is extended to a large-dimensional one by modelling the realistic airspace involving multiple traffic streams with computer-aided methodology, which is computationally expensive [19]. To resolve the diffusion problem of air traffic flow transforming between neighbouring airspace due to the introduction of the split parameters, Sun *et al.* proposed a Eulerian–Lagrangian model, which uses the real origin–destination information from the flight plan instead of the constant split parameters derived from the historical data [20–22]. Wei *et al.* and Cao *et al.* further explored the Eulerian–Lagrangian model for air traffic flow prediction and management decision-making optimization [23, 24]. The main limitation of the current method is the assumption that the speed of air traffic is considered to be constant within a specified en route airspace, which means the time-invariant aggregate air traffic model ignores not only the dynamics of air traffic flow both in time and space but also the uncertainty factors like the weather and the traffic conditions.

Aimed at modelling and predicting the traffic flow in en route airspace with full consideration of the dynamics and uncertainty of the air traffic, this paper proposes a novel dynamic air traffic flow model based on the network of en route traffic flow. First, a dynamic network of en route traffic flow is developed to capture the dynamic relationship between the traffic flow and the topological structure of the airspace. To characterize the continuous and dynamic behaviour of the air traffic flow, a continuity equation for air traffic flow within a specified airspace is built based on the model of finite control volume fixed in space [25]. The continuous space is then discretized into multiple control volumes by drawing on cell transmission models [16, 17], and finally, a time-varying air traffic flow model with parameters sequentially updated based on the statistical analysis of travel time is developed in this paper. The rest of this paper is organized as follows. Section 2 builds the dynamic network based

on the geographic topological structure of the airspace system of interest and statistically analyses distributions of travel time for aircraft travelling through the segments in the airspace system. Section 3 proposes the dynamic model for the aggregated air traffic flow and develops air traffic flow prediction methods both at flight path and sector level. Section 4 presents a case study based on a real data set from Shanghai Area Control Center (SACC), and the prediction results with uncertainty limits at two levels are analysed. Finally, the conclusions are drawn in Section 5.

2. CONSTRUCTION OF DYNAMIC NETWORK FOR AIR TRAFFIC FLOW

2.1. Definitions

The air traffic flow in a specified airspace is not independent but depends upon the upstream and downstream traffic flows; thus, a network is required to describe the overall situation and the dynamics of the air traffic flow [26]. The stochastic framework-based aggregate flow models are developed on the level of sector and centre, which do not consider the air route information [5–8]. On the other hand, the Eulerian model-based ones take the links of the entry–exist points of the sector as air route, which also results in the loss of information about the actual route structure inside the sector [20–22]. Moreover, because the traffic flow is a time-varying one, a dynamic network is developed to characterize both the static topological structure of airspace [27] and the dynamic relationship between the traffic flow and the airspace, which is illustrated in Figure 1. The left part shows the actual airspace, where the black bold lines represent the boundary of the airspace system of interest; the black lines represent the boundary of the en route sectors, and the external region out of the black bold lines represents the outer airspace. The dynamic network for the air traffic flow is shown at the right part of Figure 1, with the definitions as follows:

- (1) Interface. Interfaces represent the positions where the air traffic flow transits between the airspace system of interest and the outer airspace including the external regions in both horizontal and vertical range. For example, in Figure 1, the low-altitude airspace and the terminal area below the airspace system belong to the outer airspace. F1 and F3 represent the interfaces of air traffic flow flying into the airspace system from the outer airspace, while F2 and F4 represent the interfaces of air traffic flow leaving the airspace system to the outer airspace.
- (2) Node. Nodes represent the points which connect segments in the airspace system. This paper defines the positions of the nodes as the intersections of air traffic flow and sector boundaries and the key points in the physical structure of the air route; thus, the information about the actual route structure is contained. For example, in Figure 1, the node $V_{2,4}$ represents the position where

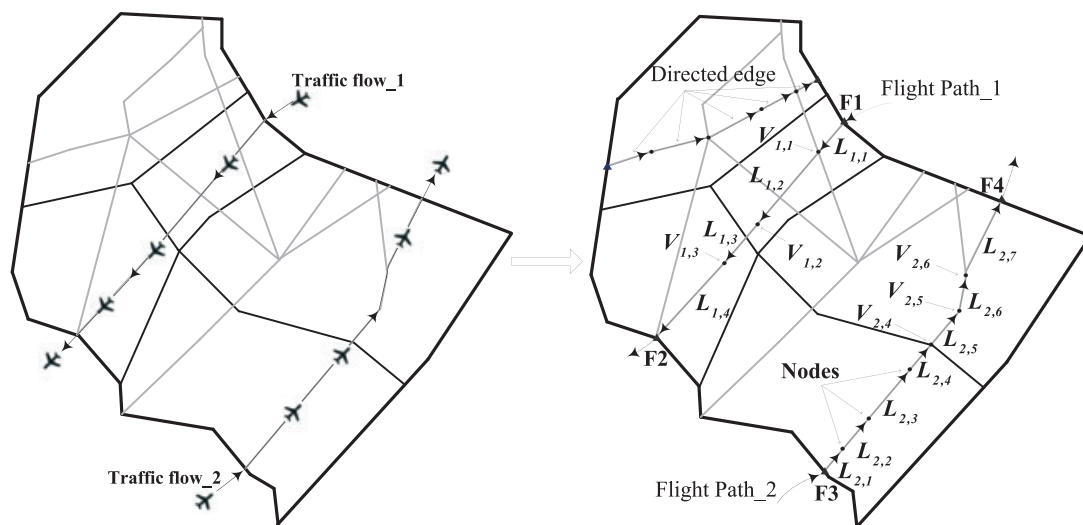


Figure 1. Air traffic flow dynamic network.

air traffic flow 2 travels through the sector boundary, while $V_{2,5}$ represents the node which is the key point in the physical structure of the air route.

- (3) Directed edge. Directed edges denote the air traffic flow between the interfaces and the nodes, where the direction of the edges is the direction of air traffic and the length of the edges is proportional to the length of the corresponding segments. For example, in Figure 1, $L_{1,1}$ represents the first segment that traffic flow 1 will travel when entering into the airspace system through the interface F1, while $L_{1,2}$ represents the second segment the traffic flow will travel.
- (4) Edge weight. Edge weight represents the weight of the directed edge, which is defined to be the travel time takes by aircraft transiting through the corresponding directed edge.

According to the definitions in the preceding texts, the dynamic network for the air traffic can be established. And then the flight path of air traffic flow can be described for simplicity of illustration as follows. As shown in Figure 1, the flight path of air traffic flow 1 can be described as air traffic flowing into the airspace system from outer airspace through interface F1, then travelling through four directed edges $L_{1,1}$, $L_{1,2}$, $L_{1,2}$, and $L_{1,4}$, and finally leaving the airspace system through interface F2; that is, flight path 1 can be denoted by $F1 \rightarrow L_{1,1} \rightarrow V_{1,1} \rightarrow L_{1,2} \rightarrow V_{1,2} \rightarrow L_{1,3} \rightarrow V_{1,3} \rightarrow L_{1,4} \rightarrow F2$, as shown at the right part of Figure 1. There are some notes as follows:

- (1) The flight time of aircraft travelling through the same segment may vary in different operational conditions, so the weight of the directed edge is dynamic. Moreover, aircraft cannot fly along the original flight path and have to reroute when affected by factors like weather and activities [28]. The segments where bad weather or special activity takes place become unavailable, and aircraft are prohibited to fly into these areas. In other words, the travel time aircraft takes to transit through these segments is infinity. Therefore, the weight of the directed edge should be set to infinity in this case and the directed edge should be deleted from the network. So, the proposed network is possible to characterize both the static topological structure of the airspace system and the dynamic relationship between the traffic flow and the airspace structure.
- (2) It can be observed from the topological structure of the network shown in Figure 1 that the reverse air route coincides with the forward one, but actually, the air traffic is separated by directions on the alternating flight levels; therefore, they are treated separately in the aggregate flow model.
- (3) The dynamic network for the en route air traffic flow proposed in this paper describes an interconnected airspace system with a user-defined size. For example, the airspace system shown in Figure 1 includes 5 sectors, 13 flight paths, 61 directed edges ($L_{1,1}$, $L_{1,2}$, ...), 12 interfaces (F1, F2, ...) and 22 nodes ($V_{2,4}$, $V_{2,5}$, ...).

2.2. Statistical analysis of the travel time

Reliable traffic flow prediction models can be built by statistical analysis of massive traffic data at a reasonable cost, both time-wise and computation-wise [29]. Based on the dynamic network of the airspace system studied in this paper, the travel time aircraft take to transit through each segment (i.e. the directed edge of the network in Section 2.1) is extracted from over 300 000 pieces of radar data to further analyse the dynamics and uncertainty both in space and time. The travel time that an aircraft takes to transit through each segment is closely related to the aircraft speed and the segment length, and it follows the rule that travel time = segment length/aircraft speed. Segment length is static data which can be obtained from National Aeronautical Information Publication, while air craft speed is dynamic.

2.2.1. Speed variation in space

For the aircraft travelling through different segments, it is obvious that the flight time varies with segment length. Additionally, the radar data analysis result indicates that the aircraft speed varies with different segments, which may also introduce uncertainty into the flight time.

To analyse the variation of the aircraft speed in different segments, the aircraft speed of eight segments is extracted from the radar data during 1 week. The result is illustrated in Figure 2, where the blue asterisks and the red triangle symbols denote the mean and the standard deviations of the speed in each segment respectively. It can be seen from Figure 2 that both the mean and the standard deviation of the speed in different segment vary significantly. The speed distribution of segment no. 6

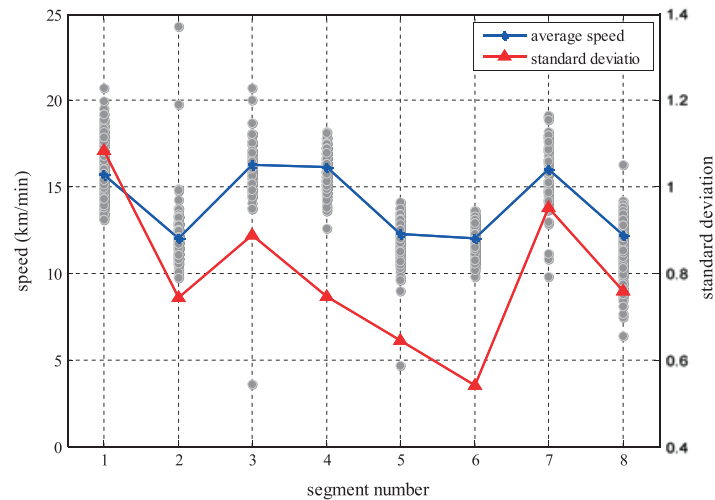


Figure 2. Aircraft speed variation in different segments.

is relatively centralized which is located mainly between 11 and 14, while that of segment no. 1 is relatively scattered from 13 to 21.

The speed variation in different segments can be finally attributed to the control actions required in the specific segments. On the one hand, for certain complicated segments with convergence or intersection points, the congestion is more likely to take place. To relieve the congestion in the airspace, the air traffic controllers may take control action to change the speed or stretch the path of the aircraft in the segment. In addition, there will be some specific control tasks required in different segments. For example, the flight level may be required to change in some segments due to the regular military flight activities, while in another case, the specific speed requirement should be met. All the control actions mentioned in the preceding texts may finally result in the speed variation in different segments.

2.2.2. Speed variation in time

For the aircraft travelling through the same segment, travel time may vary at different times for the time-varying traffic speed. Researches on highway traffic suggest that there is a linear correlation between the vehicle speed and the traffic density [30–32]. The speed of each vehicle is controlled by its driver to keep a safe distance with the vehicle ahead, and the path of the vehicle can be replanned. Different from highway traffic, the flight path, flight level and flight time information of aircraft have been given in the flight plan before departure in ATFM. Controllers (not pilots) take control actions (e.g. change aircraft speed and stretch flight path) according to the real-time overall traffic situation by taking all the aircraft in their controlled airspace into account instead of the aircraft ahead. In addition, differences in controllers' behaviour may result in different control actions for the same traffic situation, which will in turn affect aircraft speed and segment density. Therefore, the relationship between the aircraft speed and the segment density is different from that in highway traffic. To study the speed variation with time in the same segment, one segment is selected randomly from the airspace system studied in this paper. The statistical data of the speed and air traffic density obtained from the historical radar data during 1 week are presented in Figure 3.

It can be observed from Figure 3 that the grey points (i.e. aircraft speed) are scattered and show no obvious linear correlation with air traffic density. This can attribute to the dynamics and uncertainty introduced by the difference in controllers' behaviour. Figure 3 also shows that the average speed decreases slightly with the increase of the traffic density at the first stage, then followed by a rapid decrease as the traffic density continues to increase. It can be explained that, as the air traffic condition becomes more complicated during the busy hours, that is, the period of high traffic density, more control actions (such as changing the aircraft speed, stretching the flight path and holding patterns) may be required to ensure the smooth flow of air traffic, which will finally lead to the decrease of the average speed.

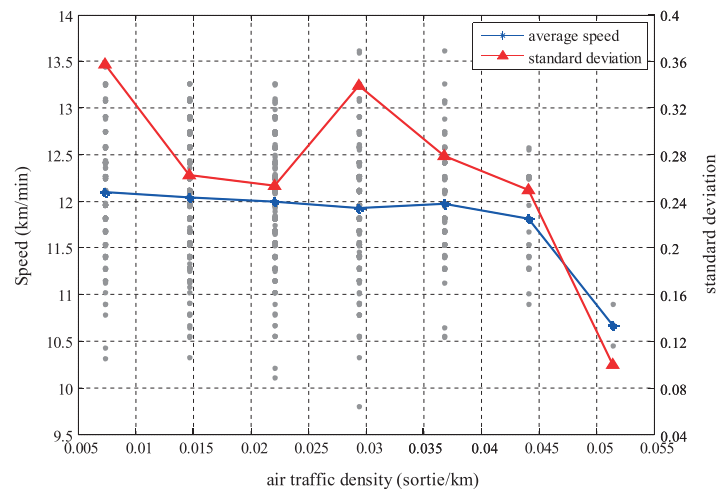


Figure 3. Aircraft speed variation for a certain segment under different traffic density conditions.

Analysis in the preceding texts indicates that travel time is affected by both spatial position and time-varying traffic density; thus, we can conclude that the travel time varies with both space and time. Therefore, we statistically analyse the distributions of the travel time for aircraft travelling through different segments under different traffic densities separately. The result of travel time for travelling through segment no. 6 under traffic density of 0.029 sorties per kilometre extracted from historical radar data is illustrated in Figure 4.

Kolmogorov–Smirnov test shows that these travel time values are well fitted in the lognormal distribution. The fitted curve is also given in Figure 4. Distributions of travel time for other segments under various traffic densities are similar, which are illustrated in Section 4.1 (we refer the reader to Figure 8 for the analysis results).

3. DERIVATION OF THE DYNAMIC AIR TRAFFIC FLOW MODEL

Based on the dynamic network developed in Section 2, a novel air traffic flow model is proposed to describe and analyse the dynamic behaviour of the traffic flow in the en route airspace of interest,

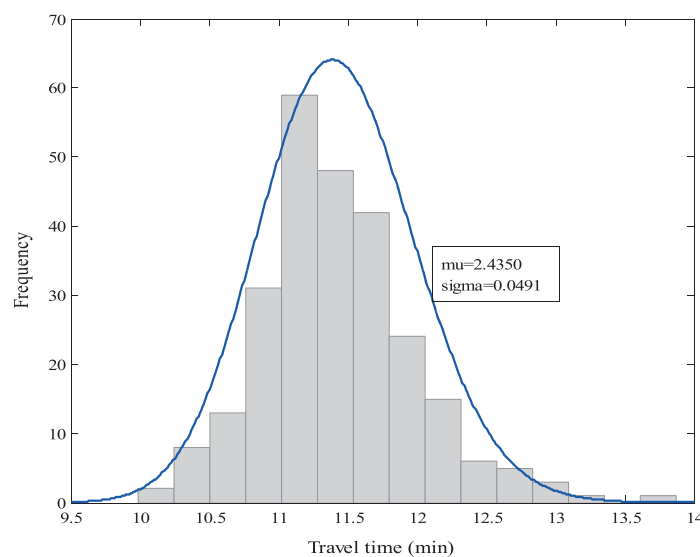


Figure 4. Analysis of travel time distribution.

which will be further applied to make short-term air traffic flow prediction. Considering the ATFM demand in China, 1 hour is selected as the short-term prediction time horizon in this study.

3.1. Modelling the en route traffic flow

This paper focuses on the aggregation of air traffic flow rather than the dynamic behaviour of individual aircraft. Therefore, the continuity equation of the finite control volume fixed in space in fluid mechanics is applied to describe the continuity behaviour of air traffic flow, and then a time-discrete and space-discrete air traffic flow dynamic model is proposed based on the space division concepts in cell transmission model which is widely used in highway traffic flow modelling.

3.1.1. Air traffic flow continuity equation

Fluid mechanical aggregation concept has been introduced into highway transportation research filed since the 1950s, which is thought as a basis for the LWR theory proposed by Lighthill, Whitham and Richards [14, 15]. A simplified LWR theory was adopted in the air transportation area by Menon to describe the traffic flow in airspace with a one-dimension partial differential equation, where they assumed that the speed of the en route air traffic is constant [18]. In practice, the speed of air traffic is not constant but varies with space and time, as analysed in Section 2.2. Therefore, considering the dynamic factors, a novel air traffic flow continuity model based on the finite control volume fixed in space is proposed in this paper, where the air traffic flow travelling through the air route is regarded as fluid. The fluid concept of air traffic is illustrated in Figure 5.

It can be seen from Figure 5 that the width of the control volume represents the width of the air route, which is normally set to 20 km, and the length and altitude range of the control volume represent the length and altitude of the corresponding air route which can be defined by users. We select an arbitrary infinitesimal element on the control volume surface, which is denoted as dS , and points in the direction out of the control volume. Then, the net traffic flow out of the infinitesimal element dS can be denoted as $\rho \mathbf{V} \cdot d\mathbf{S}$, where ρ and \mathbf{V} respectively represent the air traffic density and the flow speed at the infinitesimal element dS . It can be seen from Figure 5 that the product $\rho \mathbf{V} \cdot d\mathbf{S}$ of outflow is positive and the product $\rho \mathbf{V} \cdot d\mathbf{S}$ of inflow is negative when the flow speed \mathbf{V} points out of the control volume. The net traffic flow of the entire finite control volume can be computed by integrating the product $\rho \mathbf{V} \cdot d\mathbf{S}$ for the whole surface S , that is, $\iint_S \rho \mathbf{V} \cdot d\mathbf{S}$.

Now, consider an arbitrary infinitesimal elemental volume $d\Delta$. The mass flow of air traffic in $d\Delta$ is $\rho d\Delta$, then the total mass of the entire control volume can be calculated by the integration $\iiint_{\Delta} \rho d\Delta$. Therefore, the time rate of the mass increase inside the finite control volume is $\frac{\partial}{\partial t} \iiint_{\Delta} \rho d\Delta$.

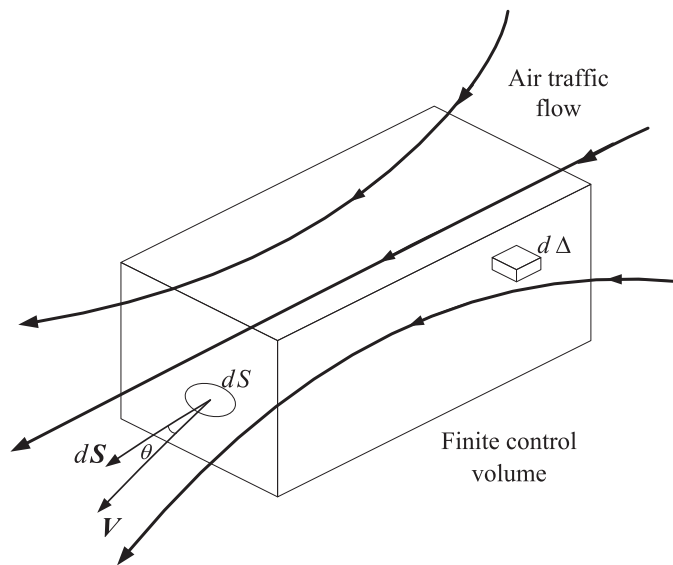


Figure 5. Air traffic flow continuity model.

According to the mass flow conservation principle, the net flow of air traffic out of the entire finite control volume equals the time rate of the decrease of mass flow in it, that is,

$$\iint_S \rho \mathbf{V} \cdot d\mathbf{S} = -\frac{\partial}{\partial t} \iiint_{\Delta} \rho d\Delta \quad (1)$$

or

$$\frac{\partial}{\partial t} \iiint_{\Delta} \rho d\Delta + \iint_S \rho \mathbf{V} \cdot d\mathbf{S} = 0 \quad (2)$$

Equation (2) is an integration form of the air traffic flow continuity equation, which is derived from the model of the finite control volume fixed in space in fluid mechanics [25]. Assuming that the observation of mass flow of air traffic in the control volume at the initial time t_0 is Q_0 , the traffic flow at an arbitrary time t_k can be expressed as follows:

$$Q_k = Q_0 - \int_{t_0}^{t_k} \iint_S \rho(t) \mathbf{V}(t) \cdot d\mathbf{S} dt \quad (3)$$

3.1.2. Dynamic model for en route air traffic

To count the number of the aircraft in a specified airspace, for example, the sector being monitored by the controller, the continuity model established in the preceding texts should be discretized both in time and space. Considering the air traffic density and speed variation both in time and space, the airspace system can be treated as a dynamic system, where the space division concept of cell transmission model is introduced to describe the dynamics of air traffic flow by using the airspace control volumes [16, 17].

According to the dynamic network presented in section 2, several interconnected directed edges make up an air route, where one directed edge, that is, a segment, corresponds to one control volume. Then, the dynamic system is divided into interconnected control volumes, which are used to describe the dynamics of the air traffic. Three types of connection, that is, (i) simile connection, (ii) convergent connection and (iii) divergent connection, are defined to characterize the traffic flow distribution among the adjacent control volumes.

The simple connection is shown in Figure 6, where the aircraft entering one volume are all from the upstream one and will all fly into the downstream one. For simplification, the continuity model is discretized in terms of segment ($i = 1, 2, 3, \dots$) in space and in terms of Δt time interval ($k = 1, 2, 3, \dots$) in time to capture the dynamics of the air traffic. Thus, the speed and density of aircraft in one specific control volume corresponding to one segment are calculated as follows:

$$\rho_i(k) = x_i(k) / L_i \quad (4)$$

$$v_i(k) = L_i / T_i(k) \quad (5)$$

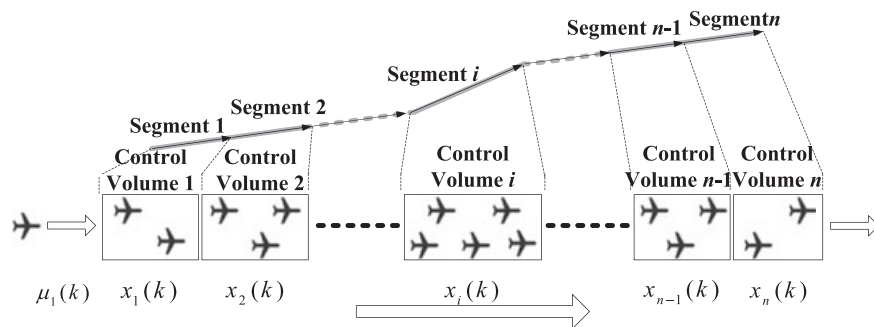


Figure 6. The simple connection among adjacent control volumes.

where $\rho_i(k)$ and $v_i(k)$ are the air traffic density and speed of the i th control volume at the k th time interval respectively; L_i is the length of the air route segment that corresponds to the i th control volume, which can be obtained from the National Aeronautical Information Publication; and $T_i(k)$ is the travel time that aircraft take to transit through the i th control volume at the k th time interval.

Based on the analysis in section 2, we assume that the travel time $T_i(k)$ for i th control volume is subject to a lognormal distribution, which is determined by the traffic density of the i th control volume at the k th time interval, that is,

$$T_i(k) \sim \ln N(\mu_{\rho_i(k)}, \sigma_{\rho_i(k)}^2) \quad (6)$$

where the parameters of the lognormal distribution, that is, $\mu_{\rho_i(k)}$ and $\sigma_{\rho_i(k)}$, are extracted from the historical radar data. Then, Equation (2) can be further expressed as the discrete-time and discrete-space difference equation combined with Equations (4) and (5),

$$\begin{aligned} x_i(k+1) - x_i(k) &= \rho_{i-1}(k)v_{i-1}(k) - \rho_i(k)v_i(k) = x_{i-1}(k)/T_{i-1}(k) - x_i(k)/T_i(k), i \in [2, n], \text{ i.e.} \\ x_i(k+1) &= x_i(k) + x_{i-1}(k)/T_{i-1}(k) - x_i(k)/T_i(k), i \in [2, n] \\ \text{or} \\ x_i(k+1) &= (1 - 1/T_i(k))x_i(k) + (1/T_{i-1}(k))x_{i-1}(k), i \in [2, n] \end{aligned} \quad (7)$$

Now, considering the first control volume, that is, $i = 1$, there is

$$x_1(k+1) = (1 - 1/T_1(k))x_1(k) + \mu_1(k) \quad (8)$$

where $\mu_1(k)$ is the system input, which denotes the number of aircraft entering the airspace system through the first control volume from outer airspace during the time interval from k to $k+1$.

The convergent connection and divergent connection are illustrated in Figure 7.

For convergent connection shown in Figure 7a, the aircraft entering one control volume (e.g. volume p) are from more than one upstream control volumes (e.g. control volume $p-1$ and j) and the outer airspace. Therefore, the aircraft count of the p th control volume at the next time instance can be calculated as $x_p(k+1) = (1 - 1/T_p(k))x_p(k) + (1/T_j(k))x_j(k) + (1/T_{p-1}(k))x_{p-1}(k) + \mu_p(k)$, where $\mu_p(k)$ is the system input, which denotes the number of aircraft entering the airspace system through the p th control volume from outer airspace during the time interval from k to $k+1$.

For the divergent connection shown in Figure 7b, the aircraft leaving one control volume (e.g. volume e) will fly into more than one control volume (e.g. control volume $e+1$ and j) and the outer airspace. For the aircraft count of control volume, $e+1$ and j are calculated respectively by using $x_{e+1}(k+1) = (1 - 1/T_{e+1}(k))x_{e+1}(k) + q_{e \rightarrow e+1}$ and $x_j(k+1) = (1 - 1/T_j(k))x_j(k) + q_{e \rightarrow j}$, where $q_{e \rightarrow e+1} + q_{e \rightarrow j} + \gamma_e(k) = (1/T_e(k))x_e(k)$ is met. $\gamma_e(k)$ denotes the number of aircraft leaving the airspace system through the e th control volume during the time interval from k to $k+1$, and $q_{e \rightarrow e+1}, q_{e \rightarrow j}, \gamma_e(k)$ is derived from the origin-destination information in the field flight plan.

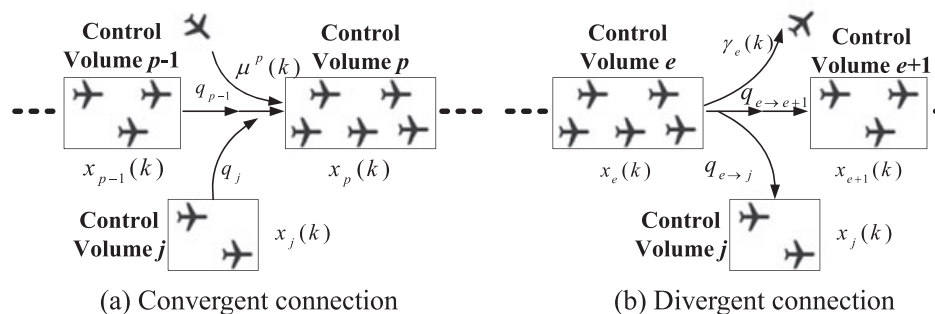


Figure 7. Convergent and divergent connections among control volumes. (a) Convergent connection and (b) divergent connection.

Equations (7) and (8) characterizing the dynamics of air traffic in one control volume now can be extended to a number of such interconnected control volumes. Define the aircraft count of each control volume in the airspace system as the state vector of the system at time step k , that is, $\mathbf{X}(k) = [x_1(k) \ x_2(k) \ \dots \ x_n(k)]^T$. Define the aircraft counts entering the airspace system from outer airspace during a unit time interval from k to $k + 1$ as the system input vector, that is, $\boldsymbol{\mu}(k) = [\mu_1(k) \ \mu_2(k) \ \dots \ \mu_n(k)]^T$, where the element's superscript variable represents the no. of the control volume through which the aircraft entering the airspace system. The proposed air traffic flow model for the dynamic airspace system consisting of multiple interconnected control volumes can be built as follows:

$$\mathbf{X}(k+1) = A(k)\mathbf{X}(k) + \boldsymbol{\mu}(k) \quad (9)$$

where the $n \times n$ state transition matrix $A(k)$ is built as follows:

$$A(k) = \begin{bmatrix} 1 - 1/T_1(k) & 0 & 0 & \dots & \dots & 0 \\ 1/T_1(k) & 1 - 1/T_2(k) & 0 & \dots & \dots & 0 \\ 0 & 1/T_2(k) & & & & \vdots \\ \vdots & \vdots & \ddots & \ddots & & \vdots \\ \vdots & \vdots & & 1/T_{n-2}(k) & 1 - 1/T_{n-1}(k) & 0 \\ 0 & 0 & \dots & 0 & 1/T_{n-1}(k) & 1 - 1/T_n(k) \end{bmatrix}$$

The elements on the main diagonal (i.e. in row i and column i) are set to $1 - 1/T_i(k)$, while the elements right under the main diagonal (i.e. in row i and column $i - 1$) are denoted by $1/T_{i-1}(k)$. All the other elements are set to 0. The elements of the state transition matrix will be updated at each time step, that is, $k = 1, 2, 3, \dots$

The output of the air traffic flow model $\mathbf{Y}(k)$ is defined as the aircraft count of the user-specified airspace at the k th time interval, which is given explicitly as

$$\mathbf{Y}(k) = C\mathbf{X}(k) \quad (10)$$

where C is a $1 \times n$ vector and $C = [1 \ 1 \ \dots \ 1]$.

3.2. Predicting the en route traffic flow

Based on the dynamic air traffic flow model developed in Section 3.1, two models are proposed for short-term air traffic flow prediction at flight path and en route sector level respectively.

3.2.1. Flight path level prediction

Select m flight paths in the region as the airspace system to study, where one flight path $i (i \in [1, m])$ consists of n_i control volumes. Then, the air traffic prediction model for the flight path i is built as follows. For each time step $k \geq 1$,

$$\mathbf{Y}_i(k) = C_i \mathbf{X}_i(k) \quad (11)$$

$$\mathbf{X}_i(k) = A_i(k-1)\mathbf{X}_i(k-1) + \boldsymbol{\mu}_i(k-1) \quad (12)$$

where $\mathbf{Y}_i(k) (i \in [1, m])$ denotes the aircraft count of the i th flight path at time k ; $\mathbf{X}_i(k) (i \in [1, m])$ is an $n_i \times 1$ dimensional state vector, which denotes the aircraft counts for n_i control volumes of flight path i at time k , and we have $\mathbf{X}_i(k) = [x_{i,1}(k) \ x_{i,2}(k) \ \dots \ x_{i,n_i}(k)]^T$; $\boldsymbol{\mu}_i(k) (i \in [1, m])$ is an $n_i \times 1$ dimensional input vector, which denotes the aircraft number entering the airspace system from outer airspace during the interval from time k to $k + 1$, and we have $\boldsymbol{\mu}_i(k) = [\mu_{i,1}(k) \ \mu_{i,2}(k) \ \dots \ \mu_{i,n_i}(k)]$; $C_i (i \in [1, m])$ is a $1 \times n_i$ dimensional vector, and $C_i = [1 \ 1 \ \dots \ 1]$; $A_i(k) (i \in [1, m])$ is an $n_i \times n_i$ dimensional state transmission matrix with elements updated sequentially upon the new arrival of the prediction results.

Assume a multivariate normal distribution for the n_i dimensional state vector at time $k=0$,

$$\mathbf{X}_i(0) \sim N_{n_i}(\mathbf{m}_0, \mathbf{C}_0) \quad (13)$$

where $\mathbf{X}_i(0) (i \in [1, m])$ is the initial state vector, which denotes the aircraft counts of each control volume in the flight path i at the initial time; \mathbf{m}_0 and \mathbf{C}_0 are the mean value and the variance of $\mathbf{X}_i(0)$ respectively, which are calculated from historical radar data. Given Equation (13), the k -step-ahead prediction for the state vector $\mathbf{X}_i(k) (X_{t:t+k} | Y_{1:t})$ and the observation $\mathbf{Y}_i(k) (Y_{t:t+k} | Y_{1:t})$ of the flight path i can be calculated recursively according to Equations (11) and (12).

3.2.2. Sector level prediction

Select s en route sectors as the airspace system to study, where one en air route sector $j (j \in [1, s])$ consists of m^j flight paths and one flight path $p (p \in [1, m^j])$ in the sector j consists of n_p^j control volumes. The air traffic prediction model for air route sector j is given as follows. For each time step $k \geq 1$,

$$\mathbf{Y}^j(k) = \mathbf{C}^j \mathbf{X}^j(k) \quad (14)$$

$$\mathbf{X}^j(k) = \mathbf{A}^j(k-1) \mathbf{X}^j(k-1) + \boldsymbol{\mu}^j(k-1) \quad (15)$$

where $\mathbf{Y}^j(k) (j \in [1, s])$ denotes the aircraft count of the en route sector j at time k ; $\mathbf{X}^j(k) (j \in [1, s])$ is an $m^j \times 1$ state vector, which denotes the aircraft counts for m^j flight path in the en route sector j , and we have $\mathbf{X}^j(k) = [X_1^j(k) X_2^j(k) \cdots X_{m^j}^j(k)]^T$; $\mathbf{X}_p^j(k) (p \in [1, m^j])$ is the aircraft counts for n_p^j control volumes of flight path p in the en route sector j , and we have $\mathbf{X}_p^j(k) = [x_{p,1}^j(k) \cdots x_{p,n_p^j}^j(k)]^T$; $\boldsymbol{\mu}^j(k) (j \in [1, s])$ is the $m^j \times 1$ dimensional input vector, which denotes the aircraft counts entering the m^j flight paths in the en route sector j from outer airspace during the time interval from k to $k+1$, and we have $\boldsymbol{\mu}^j(k) = [\mu_1^j(k) \mu_2^j(k) \cdots \mu_{m^j}^j(k)]^T$; $\boldsymbol{\mu}_p^j(k) (p \in [1, m^j])$ is the aircraft counts entering the p th flight path in the en route sector j from outer airspace, and we have $\boldsymbol{\mu}_p^j(k) = [\mu_{p,1}^j(k) \mu_{p,2}^j(k) \cdots \mu_{p,n_p^j}^j(k)]^T$; $\boldsymbol{\mu}_p^j(k) (p \in [1, m^j])$ is a $1 \times m^j$ vector; $\mathbf{A}^j(k) (j \in [1, s])$ is the state transmission matrix of $m^j \times m^j$ dimensional block matrix, and we have $\mathbf{A}^j(k) = \text{diag}(\mathbf{A}_1^j(k) \mathbf{A}_2^j(k) \cdots \mathbf{A}_{m^j}^j(k))$; $\mathbf{A}_p^j(k) (p \in [1, m^j])$ is the $n_p^j \times n_p^j$ dimensional matrix with elements updated sequentially once the new prediction results are obtained.

Assume a normal prior distribution for the m^j dimensional state vector at time $k=0$:

$$\mathbf{X}^j(0) \sim N_{m^j}(\mathbf{m}_0, \mathbf{C}_0) \quad (16)$$

where \mathbf{m}_0 and \mathbf{C}_0 are the expected value and the variance of the initial state vector $\mathbf{X}^j(0)$ respectively, which are statistically calculated from the historical radar data. Based on Equation (16), the k -step-ahead prediction for the state vector $\mathbf{X}^j(k) (X_{t:t+k} | Y_{1:t})$ and the observation $\mathbf{Y}^j(k) (Y_{t:t+k} | Y_{1:t})$ of the en route sector j can be calculated recursively according to Equations (14) and (15).

4. CASE STUDY

A case study was carried out based on a historical operation data set from SACC to verify the developed air traffic short-term prediction method. In the case study, a dynamic network of five interconnected en route sectors at altitude of 7800 m and above is constructed according to section 2.1, which consist of 13 flight paths and 61 control volumes. The air traffic flow in the next 1 hour for the 13 flight paths and 5 en route sectors in the airspace system are predicted at each time step of 1 minute, and the model parameters, that is, the elements of the state transition matrix, are updated

synchronously. The procedure in the preceding texts is repeated until the air traffic flow prediction results for 24 hours are obtained.

There are two kinds of parameters in the proposed prediction model, that is, (i) the system input $\mu(k)$ and (ii) the state transition matrix $A(k)$. The system input $\mu(k)$ is obtained from the SACC ATFM tool, where the number of the aircraft entering the airspace system in the next 1 hour can be extracted from the flight dynamic data. As for the parameters' transmission matrix whose elements consist of the variables of travel time for different segments at various time, it is impossible to update the travel time in a closed form as analysed in Section 2.2 by taking the dynamics and uncertainty of the air traffic into account. So, we have to resort to simulation-based methods, for example, Monte Carlo methods [33], to update travel time for different segments under time-varying traffic densities. The short-term prediction for the air traffic flow is given by the following procedure:

Procedure. Short-term prediction.

For $l = 1, 2, \dots, 10000$ (10000 MC iterations)

For $h = 1, 2, \dots, 24$ (24 hours)

Initialization, $k = 0$;

For $k = 1, 2, \dots, 60$ (short-term with one-minute time step)

Compute $X(k)$ and $Y(k)$ according to Equation (11)(12) or (14)(15)

For $i = 1, 2, \dots, n_i$ or m^j

Sample $T_i(k) \sim \text{In } N(\mu_{p_i(k)}, \sigma_{p_i(k)}^2)$

Update the state transition matrix $A(k)$

4.1. Flight path level traffic flow forecast

To predict the air traffic flow of the next hour at the flight path level, an air traffic flow dynamic model for each flight path in the airspace system is built according to Section 3.2.1. In addition, a statistical analysis of travel time is conducted based on the radar data and the flight plan during the past 1 week, from which the distributions of the travel time through each control volume under different traffic densities are obtained. For example, Figure 8 shows the lognormal distributions of the travel time through a certain control volume under the traffic densities of 0.0147 and 0.0515 (sorties per kilometre) respectively. It can be seen from Figure 8 that the distributions of the travel time through the same volume vary significantly under different densities. Based on the travel time distributions, the state

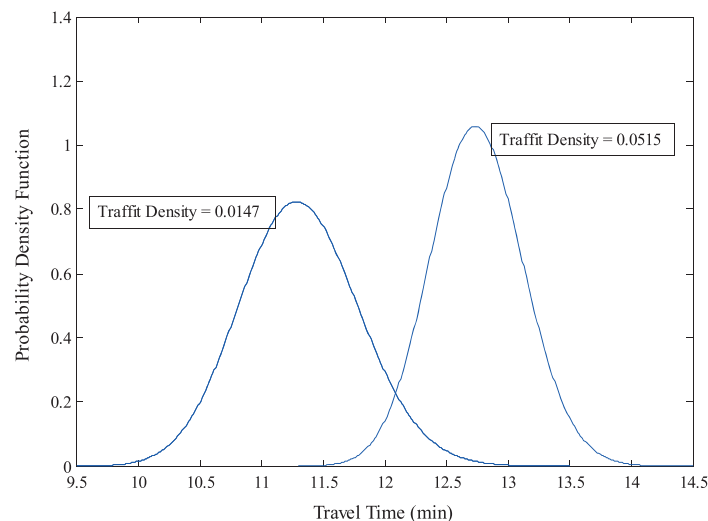


Figure 8. Lognormal distributions of the travel time.

transmission matrix in the proposed model can be updated sequentially upon the new arrival of the prediction results.

Take the no. 7 flight path of the airspace system as an example. This flight path is one of the busiest air routes in China, operating flights between Shanghai and Guangzhou directions. The traffic flow prediction results of this flight path in the next 24 hours for each 1 minute are obtained by using the procedure mentioned in the preceding texts. In order to show the results more clearly, we present part of the prediction results with 95% confidence limits for 2 busy hours (11:00–12:59), as illustrated in Figure 9. In addition, to further explore the air traffic flowing among the four control volumes of this flight path, Figure 10 shows the prediction results of each control volume and the whole flight path during 11:00 to 12:59. The solid line and the dashed line depict the mean prediction and the actual observation respectively.

It can be seen from Figures 9 and 10 that the short-term prediction results of the no. 7 flight path can well characterize the actual traffic behaviour of the flight path. One minute is selected as the time interval for modelling in order to capture the dynamics and uncertainty of the air traffic as possible. In practice, the prediction results at each minute are too redundant for air traffic controllers to keep

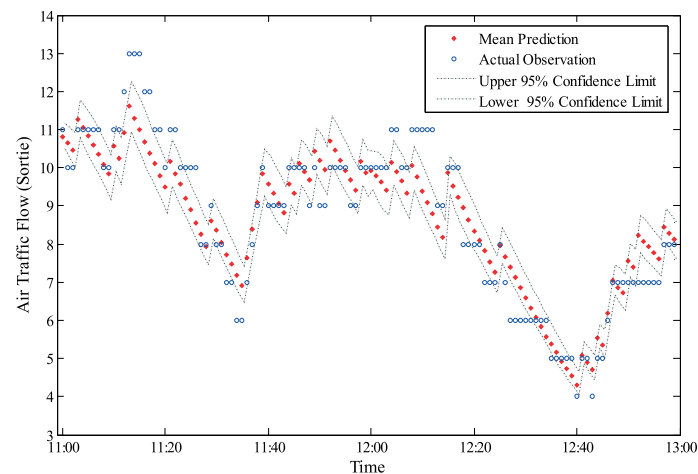


Figure 9. Air traffic flow prediction results of the no. 7 flight path.

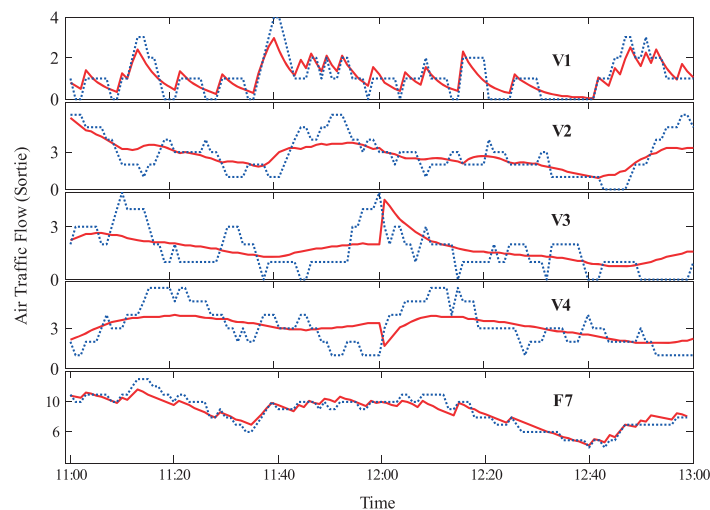


Figure 10. Air traffic flow prediction results of each control volume in flight path no. 7.

in mind. Moreover, controllers are mainly concerned about the worst traffic situation in the next 15 minutes to make sound control strategies in advance. So, 15-minute peak flow is used to trace the traffic situation of the flight path. Figure 11 shows the prediction results of the 15-minute peak flow of the no. 7 flight path in the next 24 hours.

It can be seen from Figure 11 that the prediction results for 15-minute peak flow closely approximate to the actual observations. Figure 12 presents a detailed picture of the error distribution and frequency analysis of the prediction results for flight path no. 7 during the 96 time intervals.

It can be seen from Figure 12a and c that the errors of the air traffic flow prediction results for flight path no. 7 wave around 0 and most of them fall in the interval $(-1, 1)$. Figure 12b and d also shows that the absolute errors of nearly 95% of all the 96 prediction results are within 1. The results for the other

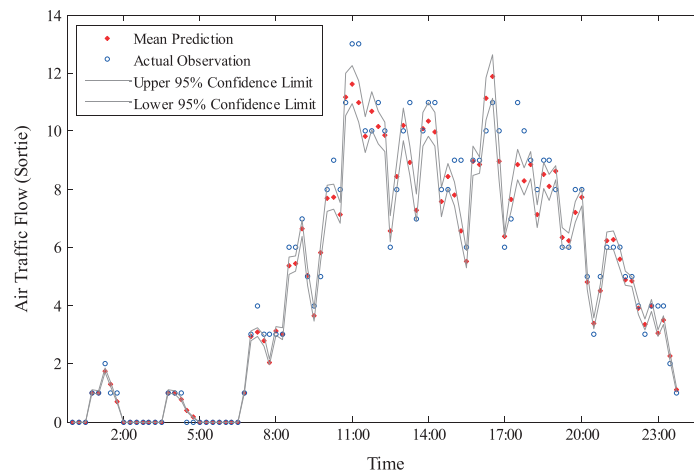


Figure 11. Prediction results for 15-minute peak flow of flight path no. 7.

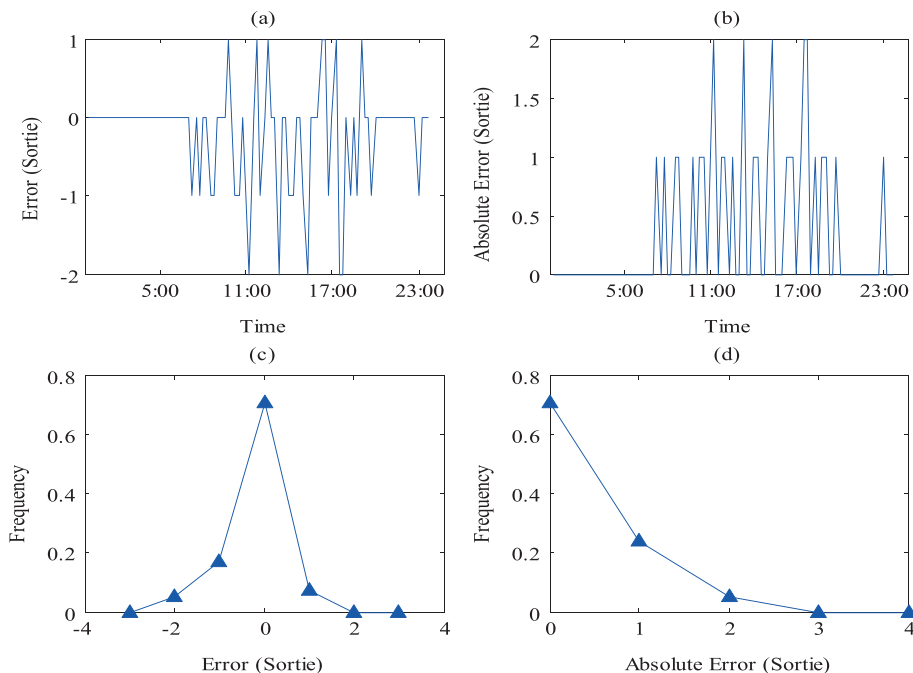


Figure 12. Error analysis of the prediction results for flight path no. 7.

12 flight paths in the airspace system are similar, and the detailed prediction error analysis will be presented in Section 4.3.

4.2. Sector level traffic flow forecast

In this section, a dynamic air traffic flow aggregate model for en route sector level is established according to section 3.2.2. Taking sector no. 4 in the airspace system as an example, the traffic flow prediction results in the next 24 hours for each 1 minute are obtained by using the proposed method. In order to show the results more clearly, we present part of the prediction results with 95% confidence limits for only 2 busy hours (18:00–19:59), as illustrated in Figure 13. The prediction results of 15-minute peak flow in the next 24 hours are presented in Figure 14.

It can be observed that the prediction results of sector no. 4 fit the actual observations quite well. To observe the prediction accuracy more clearly, Figure 15 shows a detailed picture of error distribution and frequency analysis for sector no. 4 during 96 time intervals.

It can be seen from Figure 15a and c that the errors between the prediction results and the actual observations wave around 0 and all of them fall in the interval $(-2, 2)$. Figure 15b and d also shows that the absolute errors of over 90% of all the 96 intervals are within 1 and that all of them are within 2. The

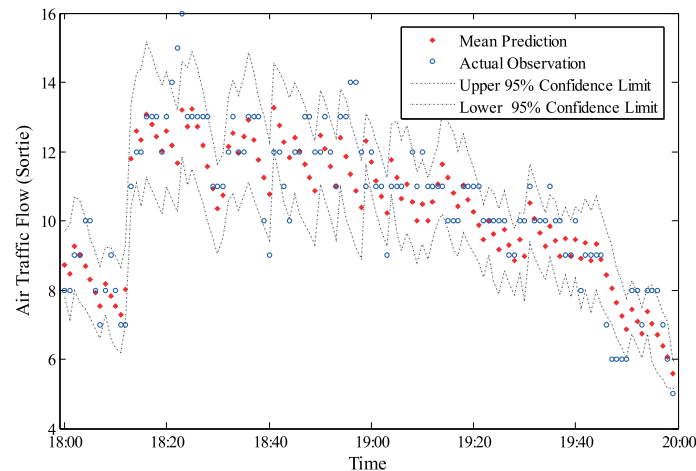


Figure 13. Air traffic flow prediction results of sector no. 4.

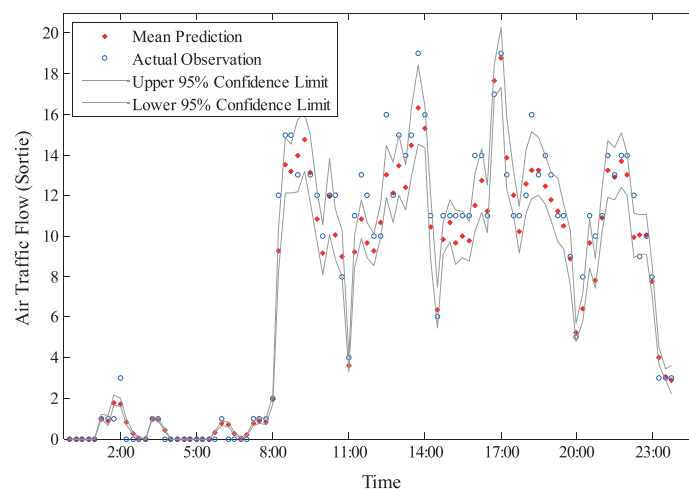


Figure 14. Prediction results for 15-minute peak flow of sector no. 4.

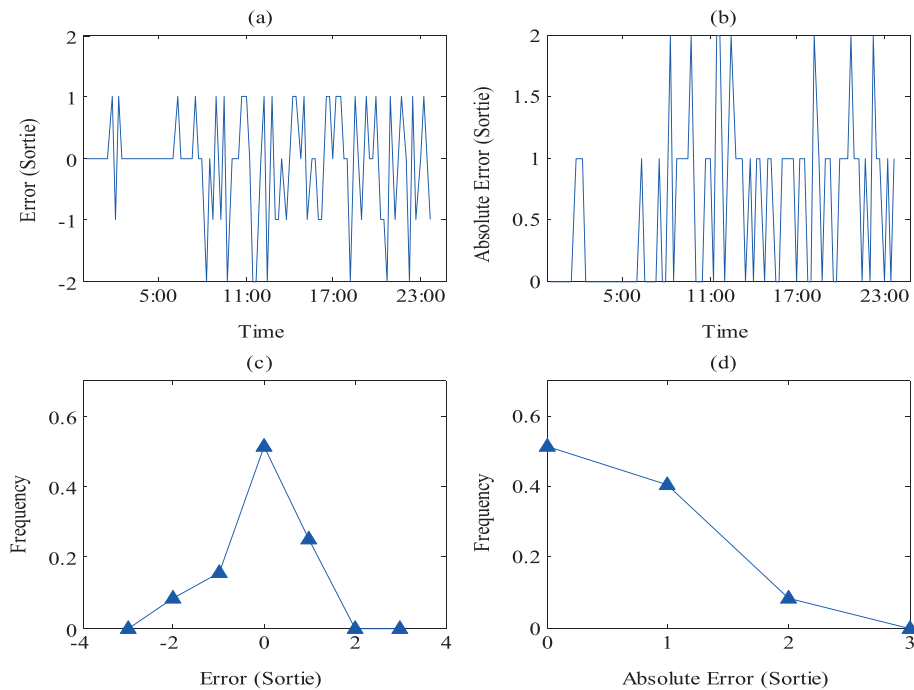


Figure 15. Error analysis of the prediction results for en route sector no. 4.

results for the other four sectors in the airspace system are similar, and the detailed prediction error analysis will be presented in Section 4.3.

4.3. Error analysis

To quantify the prediction accuracy of the air traffic flow short-term prediction method proposed in this paper, we analyse the prediction errors from both flight path and en route sector perspective. Table I shows the absolute error distributions of 13 flight paths in the airspace system.

It can be seen from Table I that the absolute errors of 13 flight paths fell in the range of 0 to 1 in more than 95% time intervals and that all the absolute errors are within 2 sorties. The analysis of the prediction errors of the 13 flight paths in the airspace system is given in Table II.

From the results listed in Table II, we can see that the mean absolute errors and the mean relative errors of the prediction results for 13 flight paths are all within 0.4 and 0.1 respectively. The normalized standard deviations of the absolute errors which reflect the prediction stability fell in 0.07 to 0.2, except for flight nos 9 and 10 whose results exceed 0.3. We can find that the air traffic flow of these two flight paths is very small, where the average observations of the 96 time intervals are only 0.6146 and 0.7083 respectively, and the maximum observations are only 3 and 4 respectively. Small prediction errors may cause big stability fluctuations in the condition of low traffic flow.

Now, considering the prediction results for en route sector level, Figure 16 shows the absolute error distributions of five sectors in the airspace system.

Table I. Absolute error distributions of 13 flight paths.

Absolute error (sortie)	Cumulated probability												
	No. 1	No. 2	No. 3	No. 4	No. 5	No. 6	No. 7	No. 8	No. 9	No. 10	No. 11	No. 12	No. 13
0	0.76	0.78	0.84	0.92	0.86	0.78	0.71	0.75	0.95	0.94	0.79	0.81	0.70
≤ 1	0.99	1.00	1.00	1.00	1.00	0.99	0.95	1.00	1.00	1.00	0.98	1.00	0.98
≥ 2	1.00	1.00	1.00	1.00	1.00	1.00	1.00	1.00	1.00	1.00	1.00	1.00	1.00

Table II. Prediction error analysis of 13 flight paths.

Flight path number	Mean observation (sortie)	Maximum observation (sortie)	MAE (sortie)	MRE	Standard deviation of absolute errors (σ) [*]	Normalized σ ^{**}
1	2.8333	9	0.2500	0.0882	0.4564	0.1611
2	2.4167	8	0.2188	0.0905	0.4134	0.1711
3	1.7708	6	0.1563	0.0882	0.3631	0.2050
4	1.5938	5	0.0833	0.0523	0.2764	0.1734
5	1.8229	6	0.1354	0.0743	0.3422	0.1877
6	2.8854	11	0.2292	0.0794	0.4444	0.1540
7	5.1667	13	0.3438	0.0665	0.5742	0.1111
8	2.6458	7	0.2500	0.0945	0.4330	0.1637
9	0.6146	3	0.0521	0.0847	0.2222	0.3615
10	0.7083	4	0.0625	0.0882	0.2421	0.3417
11	3.2708	8	0.2292	0.0701	0.4672	0.1429
12	3.0729	9	0.1875	0.0610	0.3903	0.1270
13	6.5625	18	0.3229	0.0492	0.5102	0.0777

Note:

MAE, mean absolute error; MRE, mean relative error.

^{*}The standard deviation of absolute errors is used to characterize the dispersion of the absolute errors.

^{**}The normalized standard deviation of absolute error is the ratio of σ to the mean observation, which reflects the prediction stability.

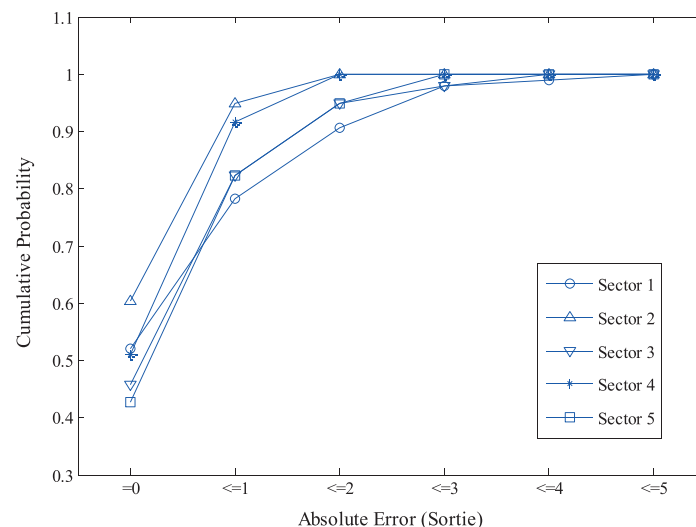


Figure 16. Prediction error distributions for five air route sectors.

It can be seen from Figure 16 that the absolute errors of sector nos 2 to 5 fell in the range of 0 to 2 in more than 95% time intervals and that the absolute errors of sector no. 1 are within 2 in more than 90% time intervals and within 3 in more than 97% time intervals. It is because the size of sector no. 1 is

Table III. Prediction error analysis of five air route sectors.

Sector number	Mean observation (sortie)	Maximum observation (sortie)	MAE (sortie)	MRE	Standard deviation of absolute errors (σ)	Normalized σ
1	9.2292	19	0.8229	0.0892	1.0801	0.1170
2	5.5521	12	0.4479	0.0807	0.5928	0.1068
3	7.1146	16	0.7917	0.1113	0.9233	0.1298
4	7.7917	19	0.5729	0.0735	0.6414	0.0823
5	6.0938	14	0.8021	0.1316	0.8493	0.1394

MAE, mean absolute error; MRE, mean relative error.

bigger than the other 4 sectors and that the average flow of sector no. 1 is 1.67 times that of sector no. 2. To quantify the prediction results, the prediction errors of the 5 sectors in the airspace system are given in Table III.

It can be observed that the mean absolute errors of the prediction results of the five sectors are all within 1 and that the average relative errors are all within 0.14. The normalized standard deviations of the absolute errors fall in the range of 0.08 to 0.14 which indicate good prediction stability.

5. CONCLUSIONS

In this paper, we address the problem of short-term air traffic flow prediction for en route airspace with an aggregated approach. A novel network-based air traffic flow model is established to characterize the dynamics and uncertainty of the en route traffic in practice. The statistical properties of the travel time through the segments are studied from the real data, based on which the state transmission matrixes are updated synchronously once the new prediction results are obtained.

This paper makes two new contributions to the field of air traffic flow prediction. First, a dynamic network of air traffic flow is constructed to characterize both the static topology of the airspace and the dynamics of the traffic flow in practice, which provides a mechanism to capture the variation of the aircraft speed both in time and space in the airspace system of interest. The travel time through a segment, that is, the edge weight in the network, under different traffic conditions is statistically analysed based on the historical radar data, which facilitate the network to take the dynamics of the en route traffic into account. Second, a novel dynamic air traffic flow model is developed based on the network with the model parameters recursively updated upon the arrival of new prediction results; thus, a more practical prediction model is obtained which takes into account the dynamics and uncertainty of the air traffic.

The proposed method is applied to a real radar data set of en route airspace. The prediction results show that our method can well track the dynamic air traffic with the mean relative prediction errors less than 0.10 and 0.14 for the flight path and en route sector level respectively. This can be attributed to the air traffic flow network and the dynamical process modelling, which facilitate the incorporation of the dynamics and the statistical properties of the air traffic flow.

6. LIST OF SYMBOLS AND ABBREVIATIONS

ATFM	air traffic flow management
SACC	Shanghai area control center
MAE	mean absolute error
MRE	mean relative error

ACKNOWLEDGEMENTS

This work was supported by the key project for Civil Aviation Joint Research Fund of National Natural Science Foundation of China (U1333202).

REFERENCES

1. Department of Development and Planning of CAAC, *Statistics of Civil Aviation 2014*, China civil aviation press: Beijing, 2015.
2. Airbus, "Airbus Global Market Forecast 2015–2034", <http://www.airbus.com/company/market/forecast/>.
3. Gong C, McNally D. A methodology for automated trajectory prediction analysis, in proceedings of the AIAA Guidance Navigation and Control Conference and Exhibit, pp.1–14, Providence, Rhode Island, USA, 2004.
4. Lymporopoulos I, Lygeros J, Lecchini A. Model based aircraft trajectory prediction during takeoff. In *Proceedings of the AIAA Guidance Navigation and Control Conference and Exhibit* Keystone: Colorado, USA, 2006.
5. Sridhar B, Soni T, Sheth K, Chatterji G. An aggregate flow model for air traffic management, in proceedings of the AIAA Guidance, Navigation, and Control Conference and Exhibit, Providence, Rhode Island, USA, 2004: pp. 1–9.
6. Sridhar B, Soni T, Sheth K, Chatterji GB. Aggregate flow model for air-traffic management. *Journal of Guidance, Control, and Dynamics* 2006; **29**: 992–997.

7. Sridhar B, Chen NY, Ng HK. An aggregate sector flow model for air traffic demand forecasting. In Proceedings of the 9th AIAA Aviation Technology, Integration, and Operations Conference, Hilton Head, South Carolina, USA, 2009; pp. 1–12.
8. Gilbo E, Smith S. A new model to improve aggregate air traffic demand predictions. In Proceedings of the AIAA Guidance, Navigation and Control Conference. Hilton Head, South Carolina, USA, 2007; pp. 1–11.
9. Bloem M, Sridhar B. Optimally and equitably distributing delays with the aggregate flow model. In Proceedings of the 27th Digital Avionics Systems Conference, St. Paul, Brazil, 2008; pp. 1–14.
10. Sridhar B, Shon R. Modeling and optimization in traffic flow management. *Proceedings of the IEEE* 2008; **96**: 2060–2080.
11. Grabbe S, Sridhar B. Congestion management with an aggregate flow model. In Proceedings of the AIAA Guidance, Navigation, and Control Conference and Exhibit. San Francisco, California, USA, 2005; pp. 1–14.
12. Andreatta G, Dell’Omo PLulli G. An aggregate stochastic programming model for air traffic flow management. *European Journal of Operational Research* 2011; **215**: 697–704.
13. Bayen AM, Raffard RLTomlin CJ. Adjoint-based control of a new Eulerian network model of air traffic flow. *IEEE Transactions on Control Systems Technology* 2006; **14**: 804–818.
14. Prandtl L, Tietjens OG. *Fundamentals of Hydro- and Aeromechanics*, Dover: New York, 1957.
15. Lighthill MJ, Whitham JB. *On Kinematic Waves. I: Flow Movement in Long Rivers. II: A Theory of Traffic Flow on Long Crowded Roads*, Royal Society A, London, 1955.
16. Daganzo C. The cell transmission model, part II: network traffic, transportation research. *Part B* 1995; **29**: 79–93.
17. Zhang X, Chang GL. Optimal control strategies with an extended cell transmission model for massive vehicular–pedestrian mixed flows in the evacuation zone. *Journal of Advanced Transportation* 2014; **48**: 1030–1050.
18. Menon PK, Sweriduk GDBilimoria KD. New approach for modeling, analysis, and control of air traffic flow. *Journal of Guidance, Control, and Dynamics* 2004; **27**: 737–744.
19. Menon PK, Sweriduk GD, Lam T, Diaz GMBilimoria KD. Computer-aided Eulerian air traffic flow modeling and predictive control. *Journal of Guidance, Control, and Dynamics* 2006; **29**: 12–19.
20. Sun D, Bayen AM. Multicommodity Eulerian–Lagrangian large-capacity cell transmission model for en route traffic. *Journal of Guidance, Control, and Dynamics* 2008; **31**: 616–628.
21. Sun D, Sridhar BGrabbe SR. Disaggregation method for an aggregate traffic flow management model. *Journal of Guidance, Control, and Dynamics* 2012; **33**: 666–676.
22. Sun D, Clinet ABayen AM. A dual decomposition method for sector capacity constrained traffic flow optimization. *Transportation Research Part B* 2011; **45**: 880–902.
23. Wei P, Cao YSun D. Total unimodularity and decomposition method for large-scale air traffic cell transmission model. *Transportation Research Part B* 2013; **53**: 1–16.
24. Cao Y, Sun D. Link transmission model for air traffic flow management. *Journal of Guidance, Control, and Dynamics* 2012; **34**: 1342–1351.
25. Anderson JD. *Computational Fluid Dynamics: The Basics With Applications*, McGraw-Hill Education, 1995.
26. Schadschneider A, Knospe W, Santen LSchrechenberg M. Optimization of highway networks and traffic forecasting. *Physica A* 2005; **346**: 165–173.
27. Lordan O, Sallan JM, Escorihuela NPrieto DG. Robustness of airline route networks. *Physica A* 2016; **445**: 18–26.
28. Mukherjee A, Hansen M. A dynamic rerouting model for air traffic flow management. *Transportation Research Part B* 2009; **43**: 159–171.
29. Li L, Su XWang Y. Robust causal dependence mining in big data network and its application to traffic flow predictions. *Transportation Research Part C* 2015; **58**: 292–307.
30. Gerlough DL, Huber MJ. Traffic flow theory: a monograph. *Fuel Consumption* 1975; **1**: 5–7.
31. Hall FL, Hurdle VFBanks JH. Synthesis of recent work on the nature of speed-flow and flow-occupancy (or density) relationships on freeways. *Transportation Research Board* 1992; **12-18**.
32. Helbing D, Hennecke A, Shvetsov VTreiber M. Micro- and macro-simulation of freeway traffic. *Mathematical and Computer Modelling* 2002; **35**: 517–547.
33. Robert CP, Casella G. *Introducing Monte Carlo Methods With R*, Springer-Verlag: New York, NY, 2010.